

# Exploring Lateral Movement Coefficient's Influence on Ground Movement Patterns in Shallow Urban Tunnels

Sara Shomal Zadeh<sup>1</sup>, and Navid Joushideh<sup>1,2</sup>

<sup>1</sup>Department of Civil and Environmental Engineering, Lamar University, Beaumont, TX 77710

<sup>2</sup>Department of Civil Engineering, University of Memphis, Memphis, TN 38152

United States

---

## ABSTRACT

*In its natural state, the ground experiences geostatic stresses, which tunnel excavation disrupts, inducing both elastic and plastic deformations in the areas surrounding the tunnel. Consequently, displacements occur in the vicinity of the tunnel and at the Earth's surface. These displacements have the potential to inflict damage on existing structures and pose environmental hazards. To mitigate these adverse consequences, accurate prediction of these changes is imperative. Several factors influence these movements, with the lateral earth pressure coefficient ( $K_0$ ) being a pivotal parameter. This paper delves into the repercussions of varying  $K_0$  values on surface movements, encompassing both longitudinal and Lateral directions, within shallow urban tunnels is investigated using two excavation methods, NATM and TBM. The study leverages numerical simulations facilitated by the PLAXIS 3D TUNNEL software, with the results meticulously presented separately. The primary objective of this research is to furnish valuable insights into the intricacies of tunneling-induced ground movements, offering pragmatic implications for the field of tunnel engineering practices and the broader realm of urban infrastructure development.*

**Keywords:** Lateral Earth Pressure Coefficient, PLAXIS 3D, Shallow Tunnel, Surface Movements.

---

## 1. INTRODUCTION

Tunnel excavation at any depth within the soil leads to a change in the stress distribution system within the soil, resulting in the convergence of the tunnel face and the occurrence of deformations on the ground surface. The nature and extent of these deformations depend on various factors such as soil conditions, groundwater conditions, tunnel location, and more.

Soil conditions encompass various parameters that influence these deformations and induced stress changes, among which the lateral earth pressure coefficient ( $K_0$ ) plays a significant role. Surprisingly, in the context of tunnel construction, less attention has been paid to this parameter compared to other influential factors.

Hoek & Brown (1980) [1] compiled information on in-situ stress conditions worldwide and presented the results in Figure 1. Contrary to the common assumption, in 92% of the case studies, it was determined that the lateral earth pressure coefficient had values greater than 1. This situation arises due to various factors such as erosion, tectonic influences, non-isotropic behavior, and the discontinuity of rocks, which result in different stress distributions.

Data indicates that the accumulation of values with  $K_0 < 1$  is more prominent near the ground surface. Therefore, this issue is of great significance, especially in the context of urban tunnels constructed near the ground surface, and it warrants further investigation.

Considering this, the paper aims to study ground movements resulting from tunneling for various values of the lateral earth pressure coefficient (both smaller and larger than 1).

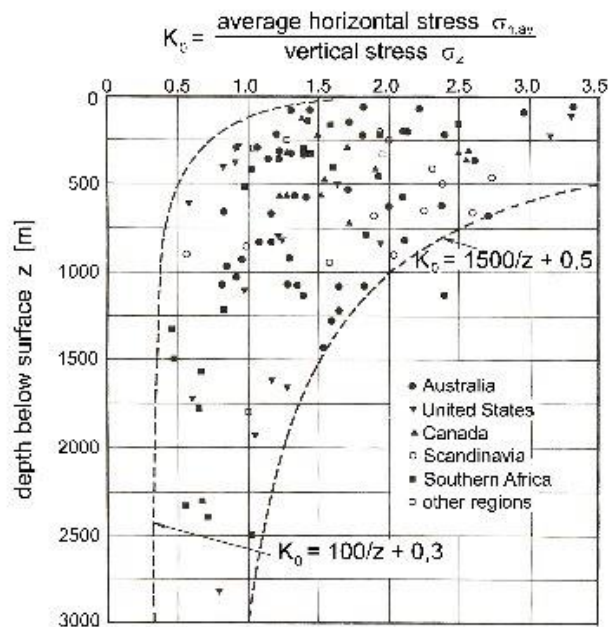


Figure 1. Vertical stresses below surface (Hoek, Brown, 1982).

## 2. LITERATURE REVIEW

Prior to this paper, several researchers have explored the influence of the lateral earth pressure coefficient ( $K_0$ ) on surface movements and structural forces during tunnel excavation. Gunn (1993) conducted tunnel construction in London clay with  $K_0=1$ , considering various soil behavior models, and compared the settlement curve with the Gaussian curve [2]. Addenbrooke and his colleagues (1997) presented a two-dimensional analysis of the Jubilee Line tunnel on James's Park Street in London, considering  $1 < K_0$ , and scrutinized the obtained results [3]. Guilloux and his team (1998) conducted studies investigating the impact of  $K_0$  on structural forces within linings [4]. Lee & Ng (2002) employed a three-dimensional analysis to simulate the Jubilee Line tunnel in James's Park Street, accounting for non-isotropic soil and varying  $K_0$  values, and compared the outcomes with the two-dimensional analysis by Addenbrook et al. (1997) [5]. Santos Pereira & Guedes (2002) compared the results of two-dimensional and three-dimensional analyses for a model with different  $K_0$  values while also examining the effect of  $K_0$  on lining structural forces [6]. Dolezalova (2002) conducted a comparative analysis, contrasting results obtained from numerical simulations with various  $K_0$  values against real on-site measurements [7]. Franzius and his colleagues (2005) conducted two-dimensional and three-dimensional analyses of the Jubilee Line tunnel in James's Park Street, considering the influence of  $K_0$  and non-isotropic soil behavior [8]. Sven Moller (2006) delved into the influence of the  $K_0$  coefficient on surface movements and lining deformation in tunnels, proposing a hypothesis that will be elaborated upon in this article [9]. Lin Chu, Bin, and their team (2007) investigated the effects of soil stratification and the  $K_0$  coefficient on parallel tunnels through physical modeling experiments [10]. Lee & Choi (2010) conducted research on the impact of the  $K_0$  coefficient on the deformation of twin tunnels [11].

In this article, we will begin by reviewing the theory put forth by Sven Moller (2006) regarding the lateral earth pressure coefficient in various scenarios. Subsequently, in the following sections, we will introduce the model, outline the modeling approach, and present the results obtained from three-dimensional analyses using the NATM and TBM methods for various values of the lateral earth pressure coefficient  $K_0$ .

### 2.1 The Role of the Lateral Earth Pressure Coefficient ( $K_0$ ) in Ground and Tunnel Deformation

The diagram below illustrates a soil element with a lateral earth pressure coefficient ( $K_0$ ) smaller than one. According to the relationship  $\sigma_v/\sigma_h = K_0$ , if  $K_0$  is less than 1, the vertical stress is greater than the horizontal stress. As evident in Figure 2, the vertical vector is larger than the horizontal vector.

The prevalence of vertical stress over horizontal stress leads to the compression of the element in the vertical direction and its elongation in the horizontal direction (the solid line represents the deformed state of the element when  $1 > K_0$ ).

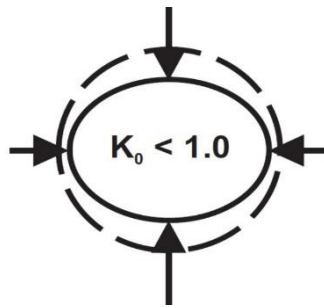


**Figure 2 - Deformation of a Soil Element under Conditions of  $1 > K_0$**

In tunnel excavation within soils where  $K_0 > 1$ , the elevated vertical stresses within the ground induce vertical movement. Consequently, the ground shifts towards the crown and invert of the tunnel, applying pressure that deflects the crown and invert inwards while pushing the tunnel sidewalls outward. This particular mechanism culminates in the creation of a settlement trough on the surface of the ground (as illustrated in Figure 3 and Figure 4). This settlement trough represents a visible depression or subsidence in the ground above the tunnel, which can potentially impact the surface infrastructure and surrounding environment. Understanding and quantifying this settlement phenomenon is crucial for tunneling projects in such soil conditions, as it has implications for structural stability and environmental considerations.

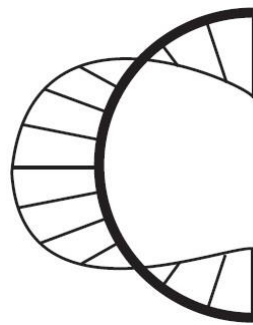


**Figure 3 - Deformation of Tunnel Walls under Conditions of  $1 > K_0$**

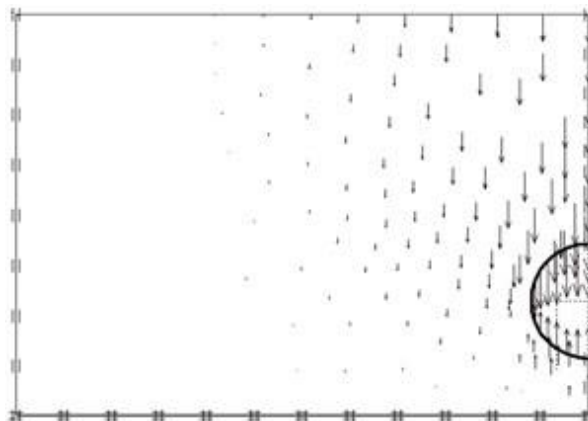


**Figure 4 - Representation of Displacement Vectors under Conditions of  $1 > K_0$**

Figure 5 illustrates a soil element with a lateral earth pressure coefficient exceeding one. In this scenario, the horizontal vector surpasses the vertical vector in magnitude. This phenomenon arises due to the relationship expressed by  $\sigma_v/\sigma_h = K_0$ , which indicates that when  $K_0$  exceeds 1, the horizontal stress prevails over the vertical stress. As a result, the element experiences compression in the horizontal direction while elongating in the vertical direction. Understanding such behavior is essential when dealing with soils exhibiting  $K_0$  values greater than 1 during tunnel excavation and construction.

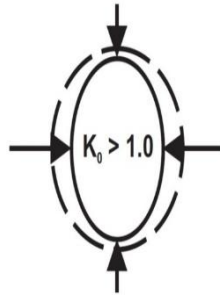


**Figure 5 - Deformation of a Soil Element under Conditions of  $1 < K_0$**

In the case of tunnel excavation in soils where  $1 < K_0$ , the highest stresses predominantly act in the horizontal direction. Consequently, this leads to horizontal ground movement. As a result, the ground shifts towards the tunnel sidewalls, applying pressure that deflects the tunnel walls inward and pushes the crown and invert of the tunnel outward. This dynamic process ultimately gives rise to an uplift or bulging on the ground surface, as illustrated in Figure 6 and Figure 7. Understanding and analyzing this phenomenon is of paramount importance for tunneling projects in soils with  $K_0$  values exceeding 1, as it has implications for both structural considerations and ground surface effects.



**Figure 6 - Tunnel Walls Deformation under Conditions of  $1 < K_0$**

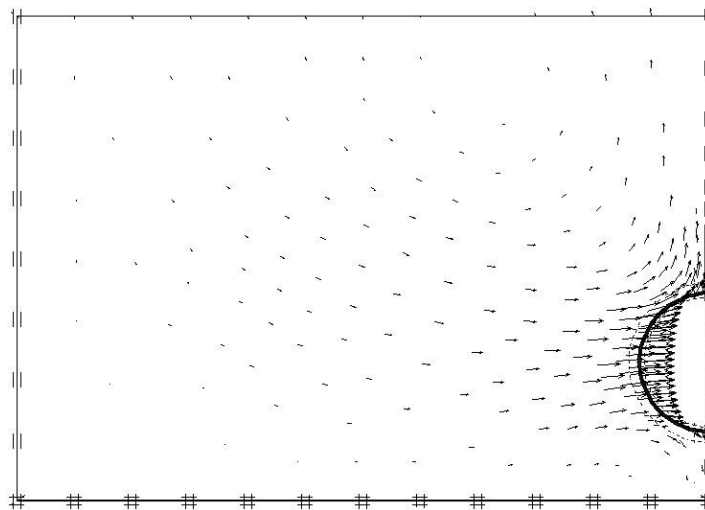


**Figure 7 - Representation of Vector Displacement under Conditions of  $1 < K_0$**

### 2.3 Modeling the Tunnel with PLAXIS 3D TUNNEL Software

PLAXIS is one of the finite element software packages with capabilities for solving various geotechnical problems. The main stages of modeling in this software for investigating soil behavior during tunnel excavation include [12]:

### 2.4 Geometric Modeling

For tunnel modeling, a tunnel with a diameter of 8 meters and a depth of 16 meters is considered. The model block has dimensions of 28 meters in height, 40 meters in width, and 100 meters in length.

To mitigate boundary effects, the initial 25 meters of the model are assumed to have undergone excavation and lining, and the excavation is examined in the region between 25 meters and 75 meters.

**2.5 Meshing**

In this modeling, triangular elements with 15 nodes are used for coarse meshing. Fine meshing is applied only in critical areas such as the ground surface, the interior of the tunnel, and the vertical cross-section above the tunnel (the tunnel's cross-sectional line). To reduce computational volume and for symmetry reasons, only half of the tunnel is modeled (as shown in Figure 8).

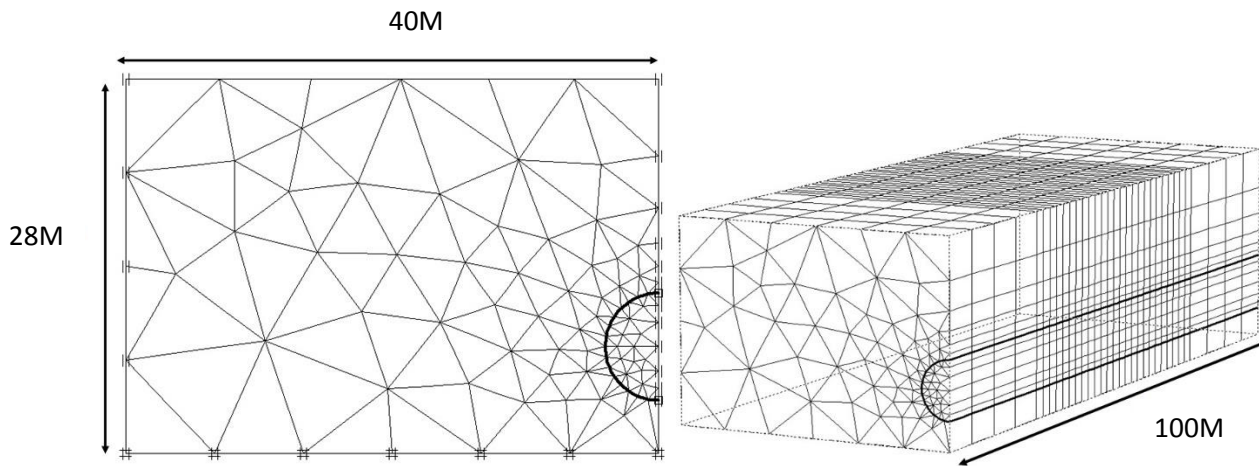


**Figure 8 - Schematic Representation of 2D and 3D Model Meshing**

By utilizing the PLAXIS 3D TUNNEL software, the complex behavior of the soil during tunnel excavation can be simulated and analyzed effectively, considering the specific geometry and boundary conditions of the tunneling project. This modeling approach allows for a comprehensive assessment of the soil's response to tunneling activities and the evaluation of potential risks and deformations.

**2.6 Geotechnical Properties of the Model**

In this article, a homogeneous soil sample is used for analysis and modeling. The mechanical properties of the soil are provided in Table 1. The Mohr-Coulomb soil behavior model has been chosen for this study. This decision is based on the model's ability to offer a more realistic representation compared to linear elastic behavior. Additionally, its parameters are more readily accessible compared to other complex behavioral models. The analysis is conducted under consolidated undrained conditions [13].

**Table 1 - Mechanical Properties of the Soil**

$\gamma$ (KN/m <sup>3</sup> )	E (KN/m <sup>2</sup> )	$\nu$ -	C (KN/m <sup>2</sup> )	$\phi$ -	$\psi$ -
19	42*10 <sup>3</sup>	0.25	20	20	0

**2.7 Three-Dimensional NATM Modeling**

The three-dimensional block is composed of numerous slices, with each slice representing a drilling step of d meters in length. This distance is excavated and lined during each cycle. In this modeling scenario, d = 2 meters has been chosen.

After establishing the initial geostatic stresses, the excavation follows these steps:

In the computational phase (i-1), the soil inside the tunnel corresponding to slice number 1 is removed.

In the subsequent phase (i), the soil inside the tunnel corresponding to slice number 2 is excavated, and lining is installed for slice number 1.

In phase (i+1), the soil related to slice number 3 is removed, and lining for slice number 2 becomes active. This process continues in the same manner in the following computational phases (refer to Figure 9). This modeling method is known as the Step-by-Step approach.

This approach allows for a detailed simulation of the excavation and lining process, enabling a comprehensive analysis of the tunnel behavior and its interaction with the surrounding soil.

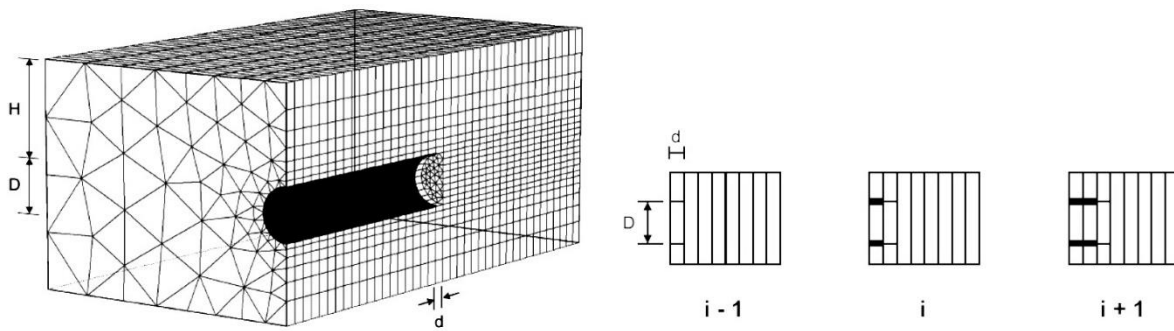


Figure 9 - Step-by-Step Excavation and Lining Process for NATM Tunneling

Table 2 - Table 2: Mechanical Specifications of Lining

Parameter	Unit	Quantity
AE	KN/m	106*6
EI	KN.m <sup>2</sup> /m	104*4.5
D	m	0.3
v	-	0
W	KN/m/m	0

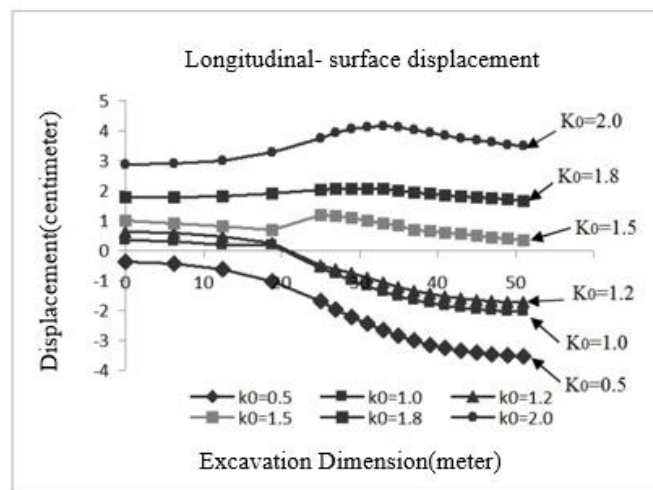


Figure 10 - Longitudinal Displacement Profiles of Three-Dimensional NATM Models

Table 3 - Maximum Longitudinal Displacement Values

Maximum Displacement (Centimeters)	Lateral Earth Pressure Coefficient
-3.52	0.5
-2.04	1
-1.72	1.2

+1.2	1.5
+2.07	1.8
+4.15	2

Lateral Displacement: Figure 11 illustrates the lateral displacement curves obtained from three-dimensional NATM analysis, considering various  $K_0$  values. As depicted in the figure, as  $K_0$  increases from values less than 1 to values greater than 1, the displacement curve gradually shifts towards shallower depths along the tunnel centerline. For values slightly greater than 1, rather than settlement, we observe uplift at the ground surface.

Table 4 provides the specific values of three-dimensional lateral displacements along the tunnel centerline for six distinct models.

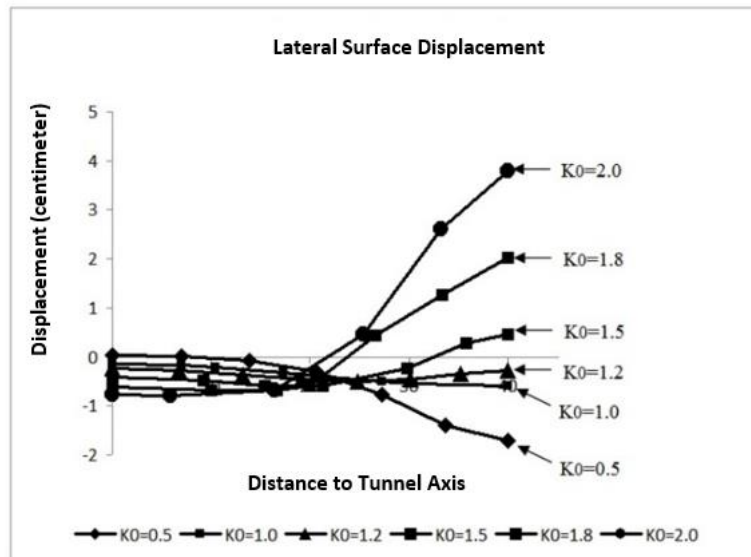


Figure 11 - Lateral Displacement Curves of Three-Dimensional NATM Models

Table 4 - Lateral Displacement Values along the Tunnel Centerline

Maximum Lateral Displacement (Centimeters)	Lateral Earth Pressure Coefficient
-1.7	0.5
-0.59	1
-0.5	1.2
+0.45	1.5
+2.02	1.8
+3.8	2

### 3 THREE-DIMENSIONAL TBM MODELING

The TBM excavation process includes the following steps:

Soil Excavation: Soil is excavated in front of the TBM, and face support pressure is applied to stabilize the excavation face. This pressure ranges between minimum and maximum values and depends on various factors such as soil type, tunnel depth, groundwater pressure, and more. Insufficient pressure can lead to soil collapse into the excavation face, while excessive pressure can result in face collapse.

Settlement Due to TBM Diameter: Since the diameter of the TBM cutterhead is larger than the tunnel, there is always some additional excavation, leading to ground settlement. Additionally, the tapered shape of the TBM body (the difference in diameter between its front and rear ends) contributes to this settlement. To simulate this settlement, a settlement coefficient is applied incrementally from the front to the rear of the TBM in successive slices.

Interaction Between Shield and Soil: The interaction between the TBM shield and the surrounding soil reduces the soil's resistance. This reduction in soil resistance is represented by a parameter known as the Reduction Coefficient ( $R_{inter}$ ), typically ranging between 0.7 and 0.8. In this model, an  $R_{inter}$  value of 0.7 is used, indicating a 30% reduction in soil resistance.

Hydraulic Jack Thrust: Hydraulic jacks apply radial pressure to install tunnel lining segments at the rear of the TBM. After installation, a new lining ring is added.

Grout Injection: Following lining installation, a void space known as the annulus exists between the lining and the ground. To prevent ground settlement, this space is filled with grout. Grout injection is simulated by applying radial pressure at the rear of the TBM at the location of the lining installation.

This simulation method is referred to as the Step-by-Step Pressure method (Figure 12) [9, 12].

The model specifications, cross-section, and excavation steps are similar to the NATM method, with the main difference being that in this model, the entire cross-section is excavated simultaneously. The mechanical properties of the lining and TBM shield are presented in Tables 5 and 6, respectively.

**Table 5 - Mechanical Specifications of the Tunnel Lining**

ID	Material Model	Material Type	$\gamma$ (KN/m3)	E (KN/m2)	$\nu$
LINING	Linear Elastic	Non-Porous	24	$10^6 \cdot 31$	0.1

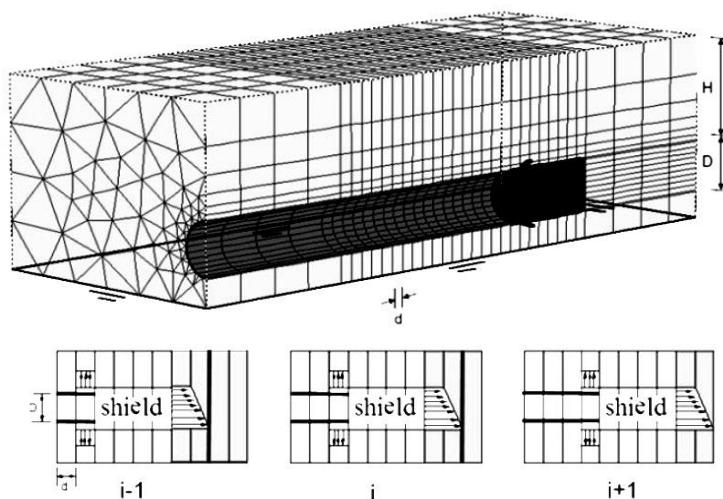


**Figure 12 - An Illustration of the Step-by-Step Pressure Method for TBM Tunneling**



Table 6 - Mechanical Specifications of the TBM Shield

ID	Material Model	AE KN/m	EI KN.m <sup>2</sup> /m	D m	W KN/m/m	v
TBM	Elastic	10 <sup>6</sup> *2.8	10 <sup>4</sup> *3.8	35.0	15.38	0

## 4 BM ANALYSIS RESULTS

### 4.1 Lateral Displacement

Longitudinal Displacement: Three-dimensional TBM analysis was conducted for six models with  $K_0$  values of 2, 1.8, 1.5, 1.2, 1, and 0.5. Figure 13 illustrates the longitudinal displacement curve along the excavation path for the initial 50 meters of the model.

For models with  $K_0$  values of 1 and 0.5, the displacement exhibits a settlement pattern, whereas for models with  $K_0$  values of 2, 1.8, 1.5, and 1.2, the displacement takes on an uplift pattern. Table 7 provides the maximum displacement values for each model.

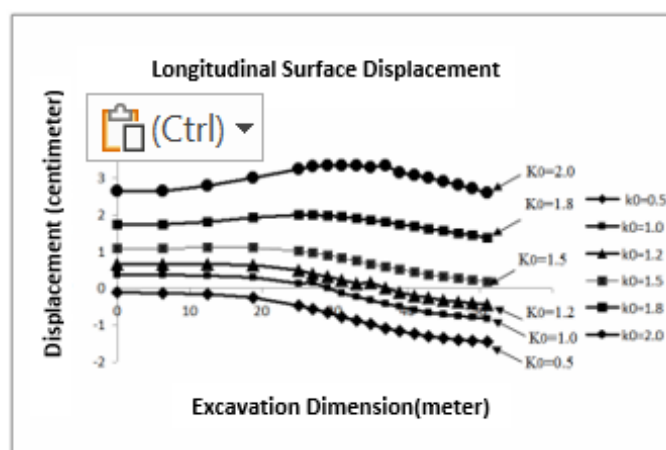


Figure 13 - Longitudinal Displacement Curves of Three-Dimensional TBM Models

Table 7 - Maximum Longitudinal Displacement Values

Maximum Displacement(centimetre)	Lateral Earth Pressure Coefficient
-1.45	0.5
-0.79	1
-0.44	1.2
+1.02	1.5
+2	1.8
+3.34	2

Lateral Displacement: Figure 14 illustrates the transverse displacement curves for three-dimensional TBM analysis at various  $K_0$  values. As depicted in the figure, the displacement curve exhibits settlement for  $K_0 < 1$  and uplift at the surface for  $1 \leq K_0$ . Table 8 presents the values of three-dimensional transverse displacements along the tunnel centerline.

Table 8 - Lateral Displacement Values

Maximum Transverse Displacement (centimetre)	Lateral Earth Pressure Coefficient
-0.46	0.5
+0.13	1
+0.48	1.2
+1.02	1.5
+2	1.8
+3.24	2

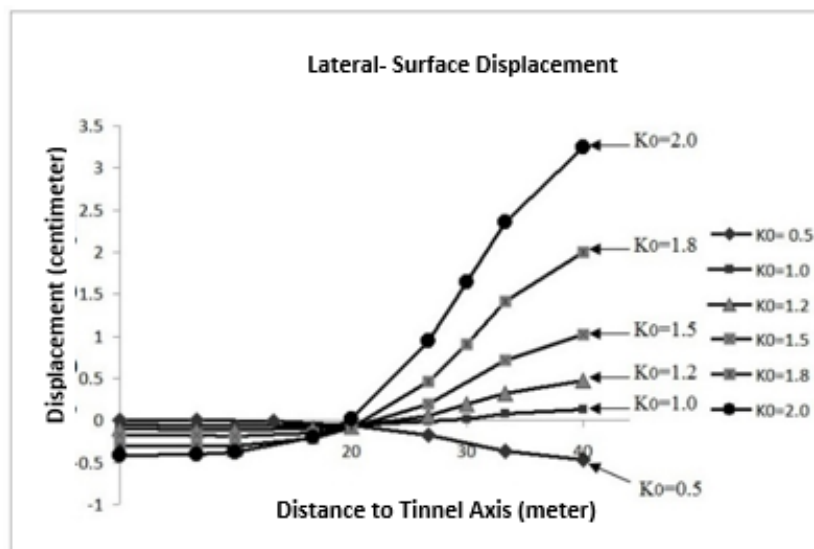


Figure 14 - Lateral Displacement Curves of Three-Dimensional TBM Models

## 5. CONCLUSION

The insightful analysis presented in this study challenges conventional assumptions about the behavior of shallow tunnel excavations. Contrary to expectations, the results indicate that shallow tunnel excavation will not always lead to settlement at the ground surface; under specific conditions, it may result in surface uplift.

The interplay between vertical and horizontal stress components, as characterized by the equation  $\sigma_v/\sigma_h = K_0$ , emerged as a pivotal factor in governing tunnel deformation patterns. When  $K_0$  surpasses 1, vertical stress dominates over horizontal stress, prompting vertical ground movement during excavation. Consequently, the tunnel crown and invert deflect inward, while the tunnel walls deflect outward, ultimately leading to subsidence at the ground surface.

Conversely, for  $K_0$  values less than 1, horizontal stress prevails over vertical stress. This results in horizontal ground movement, causing the tunnel walls to deflect inward, while the tunnel crown and invert deflect outward, leading to surface heave rather than the anticipated subsidence.

An intriguing aspect revealed in this study is the impact of the lateral earth pressure coefficient ( $K_0$ ) on longitudinal settlement. As  $K_0$  transitions from values less than 1 to values greater than 1, the longitudinal settlement curve exhibits a gradual shallowing effect. This remarkable phenomenon is accompanied by a shift from settlement to uplift behavior at the ground surface.

The maximum surface settlement obtained from various NATM analyses is 52.3 centimeters, while for TBM modeling, it is 45.1 centimeters for  $K_0 = 0.5$ . The maximum surface heave obtained from NATM analysis is 15.4 centimeters, and for TBM modeling, it is 34.3 centimeters for  $K_0 = 2$ .

Additionally, a noteworthy comparison emerged between two excavation methods—The New Austrian Tunneling Method (NATM) and Tunnel Boring Machine (TBM) excavation. Irrespective of identical  $K_0$  values, TBM excavation consistently yields

reduced surface settlement and heave compared to the NATM method. This outcome is attributed to the immediate lining installation post-excavation in the TBM method, effectively curtailing stress release and additional deformations in the surrounding soil.

The three-dimensional NATM analysis results for different  $K_0$  values show that the transverse displacement along the tunnel centerline for values  $2.1 > K_0 > 0.5$  is of the settlement type, while for values  $2 > K_0 > 0.51$ , it is of the uplift type.

The three-dimensional TBM analysis results for different  $K_0$  values show that the transverse displacement along the tunnel centerline for values  $1 > K_0$  is of the settlement type, while for values  $1 \leq K_0$ , it is of the uplift type.

These findings carry profound implications for tunnel engineering practices. Tunnel designers and engineers must exercise meticulous consideration of geological conditions, excavation methods, and the specific value of  $K_0$  when planning shallow tunnel projects. Overlooking these factors may result in unexpected and potentially costly consequences.

In conclusion, this study underscores the necessity for a nuanced understanding of the intricate relationship between geological parameters, excavation methodologies, and lateral earth pressure coefficients in shallow tunnel engineering. This understanding is pivotal for ensuring the safe and efficient execution of tunnel projects across diverse geological contexts. Future research endeavors can delve deeper into these complexities to further refine tunneling techniques and enhance the predictability of tunnel behavior in real-world applications.

## **REFERENCES**

- [1] John A. Hudson and John P. Harrison, "Engineering Rock Mechanics", an introduction to the principles, pages 59-69, Pergamon Press, Imperial College of Science, Technology and Medicine University of London, UK (1997).
- [2] M.J. Gunn, "The prediction of surface settlements profiles due to tunnelling". In G.T Housby and A.N. Schofield, editors, predictive soil mechanics: proceeding of the wroth memorial symposium, pages 304-316, London, 1993.
- [3] T.I. Addenbrooke, D.M Potts, and A.M. Puzrin. "The influence of Pre-failure soil stiffness on the numerical analysis of tunnel construction". *Geotechnique*, 47(3): 693-712, 1997.
- [4] A.H. Guilloux, H. Bissonais, J. Robert, and A. Bernardet. "Influence of the  $K_0$  coefficient on the design of tunnels in hard soils". In proc, of the world tunnel congress'98 Tunnels and Metropolises, pages 367-392, sao paulo, Brazil, 1998.
- [5] G.T.K Lee and C.W.W. Ng. "Three-dimensional analysis of ground settlement due to tunnelling : role of  $K_0$  and stiffness anisotropy". In proc Int. symp. on Geotechnical Aspect of underground construction in soft ground, pages 617-622, Toulouse, 2002.
- [6] R.J. Guedes and C. Santos Pereira. "The role of the soil  $K_0$  value in numerical analysis of shallow tunnels". In proc. Int. Symp. Geotechnical Aspects of underground Construction in soft ground, IS-Tokyo'99, pages 379-384, Tokyo, 2002.
- [7] M. Dolezalova. "Approaches to numerical modelling of ground movements due to shallow Tunnelling". In Proc, 2nd Int. Conf. On soil structure interaction in urban civil Engineering, pages 365-373, Zurich, 2002.
- [8] J.N. Franzius, D.M Potts and J.B Burland. "The influence of soil anisotropy and  $K_0$  on ground surface movements resulting from tunnel excavation". *Geotechnique*, 55(3): 189-199, 2005.
- [9] Sven Möller, "Tunnel induced Settlement and Structural forces in lining", PHD thesis, University of Stuttgart, Germany, 2006.
- [10] Chu, Bin-Lin; Hsu, Sung-Chi; Chang, Yi-Long; Lin, Yeong-Shyang. (2007). "Mechanical behavior of a twin-tunnel in multi-layered formations". *Tunnelling and Underground Space Technology*, 22, 351-362.
- [11] Choi, J.I. and S.W. Lee, "Influence of existing tunnel on mechanical behavior of new tunnel". *KSCE Journal of Civil Engineering*, 2010: p. 1-11.
- [12] R. J. B. Brinkgreve and P. A. Vermeer, "PLAXIS 3D Tunnel Tutorial Manual", Edited by Balkema Publishers. (2001).
- [13] M. Behpour Gohari, A. Rouhi Mehr, R. Vafaie pour, "PLAXIS V8", Finite Element Code for Soil and Rock Analysis, pages 27-38, Forouzesh Press, Tabriz, (1385).
- [14] S.C. Moller, P.A. Vermeer, P.G. Bonnier. (2003). "A fast 3D tunnel analysis". second MIT Conference Boston, USA.
- [15] Hoek, E. and Brown, E.T. (1980) *Underground Excavations in Rock*. Inst. Min. 537 Metall, London.